Forced convection boundary layer flow in a thin nanofluid film on a stretching sheet under the effects of suction and injection

Nur Ilyana Kamis[1], Lim Yeou Jiann[1], Taufiq Khairi Ahmad Khairuddin[1], Sharidan Shafie[1], and Md Faisal Md Basir[1*]

[1] *Department of Mathematical Sciences, Faculty of Sciences, Universiti Teknologi Malaysia, 81310, Johor Bahru, Malaysia*
[*] *Corresponding author. E-mail: mfaisalmbasir@utm.my*

Received: Dec. 06, 2021; Accepted: June 18, 2021

The forced convection thin-film hybrid nanofluid flow over a stretching sheet with heat transfer is investigated in the present study. The effect of the suction and injection is considered. The concerned hybrid nanoparticles are copper and alumina which are dissolved in blood base fluid. Suitable similarity variables are applied to convert the nonlinear governing partial differential equations subject to appropriate boundary conditions into a set of ordinary differential equations. The MATLAB solver bvp4c is utilized to solve the similarity transformed governing equations numerically. There exists a great agreement when the present computed findings are compared with the published results for a limiting condition. Dual solutions are obtained for the velocity and temperature profiles. Conflict behavior is observed for the effect of the unsteadiness parameter and mass transfer parameter on both solutions of the velocity and temperature distributions. The increment of the mass transfer parameter has enhanced the velocity profile in the injection case, while an opposite trend is detected in the suction situation.

Keywords: permeable stretching sheet; thin film, numerical; bvp4c; dual solution

http://dx.doi.org/10.6180/jase.202206_25(3).0009

1. Introduction

Recently, technological developments have driven researchers to conduct various studies to meet the needs of consumers. Heat transfer is a crucial part of certain regions like the synthetic industry, oil and gas, atomic energy, electrical energy, and so on. The investigation on the heat transfer issues over a stretching sheet from a slit has attracted the attention of scientists because of its significance in numerous modern applications. Crane [1] was the first researcher who has studied the viscous fluid flow when the sheet was stretched. The advancement of theoretical works on the boundary layer flow along with a stretching sheet has also attracted the interest of other researchers due to its wide application in the industry and engineering [2, 3].

Some scientists have been motivated to do a few examinations on a similar issue and broadened it with the nearness of a thin film. The reason behind this is that the thin-film flow has altogether added to the territory of businesses, designing, and innovation just as other developing fields of science. Wang [4] initiated a liquid film problem with an accelerated fluid flow over a stretching sheet. The nonlinear governing partial differential equations (PDEs) subjected to boundary conditions have been reduced to the nonlinear ordinary differential equations (ODEs) by employing appropriate similarity transformations.

Andersson et al. [5] imported the similarity transformation for the dimensionless temperature. Andersson et al. [5] extended the work of Wang [4] by reducing the governing time-dependent equations into ODEs with the help of the new similarity variables. These issues have been addressed by Wang [6] with the implementation of the semi-analytical method and the numerical method has been practiced by

Table 1. Thermophysical properties of the fluid

Physical property	Blood	Alumina	Copper
$C_\rho(J/kg\times)$	3617	765	385
$\rho(kg/m^3)$	1150	3970	8933
$k(W/m\times K)$	0.53	40	400

Liu and Andersson [7] and Metri et al. [8]. The presence of a couple of additional effects such as thermophoresis and constant wall temperature has given noteworthy consequences to the movement of the liquid, (see [9–12]). Santra and Dandapat [11] investigated the thin-film flow over a heated horizontal stretching plate. Further, Qasim et al. [12] had applied Buongiorno's model which incorporates the effects of Brownian motion and thermophoresis to analyze the thin-film nanofluid flow.

Hybrid nanofluid contains two distinct nanoparticles that are dissolved in the base fluid and the fluid has a better thermal conductivity as compared to the regular nanofluid. Sidik et al. [13] claimed that higher thermal properties are produced with the presence of hybrid nanoparticles as compared to the fluid with a single nanoparticle in the base fluid. Bvp4c is a package in MATLAB programming and generally be utilized to solve heat transfer problems. According to Afonso and Vasconcelos [14], bvp4c is a boundary value problem solver with a fourth-order accuracy function that implements the Lobatto IIIa formula which is a kind of collocation method. Afonso and Vasconcelos [14] had tested the capacity and productivity of the solver via certain cases of boundary value problems. Sulochana and Sandeep [15] applied the bvp4c to investigate the characteristic of velocity and temperature for the copper-water nanofluid.

The main aim of the present study is to obtain the numerical simulation of the heat transfer in a thin film hybrid nanofluid flow over an unsteady permeable stretching sheet. The governing equations of the fluid problem in the form of PDEs are transformed into a set of ODEs by implementing the similarity transformations that were proposed by Wang [6]. The nanoparticles alumina and copper in blood as a base fluid are considered. MATLAB solver bvp4c is applied to compute the numerical solutions of the concerned fluid problem. Then, the influence of the pertinent parameters on the velocity and temperature profiles are graphically displayed and discussed.

2. Materials and method

Consider two-dimensional incompressible thin-film hybrid nanofluid over an unsteady permeable stretching sheet with the suction and injection conditions. The horizontal plane of the sheet is placed at the $x-$axis from the narrow slit and y is perpendicular to it. The fluid flows over a horizontal plane with stretched velocity $U_w(x,t) = bx(1-\alpha t)^{-1}$ in which $b > 0$ (stretching rate), $\alpha > 0$. The problem is valid only for $\alpha t < 1$ as depicted in Fig. 1 [6]. The porous boundary layer is sucked, $V_w > 0$ and injected, $V_w < 0$ with velocity $V_w = (V_w)_0 (1-\alpha t)^{-\frac{1}{2}}$ where $(V_w)_0$ is an initial concentration of the reactant species. The surface temperature for slit and reference is defined as $T_w(x,t) = T_0 + T_{ref}\left[\frac{bx^2}{2v}\right](1-\alpha t)^{-\frac{3}{2}}$ [6]. Then, the governing equations in the form of unsteady thin-film flow are as follows [16]:

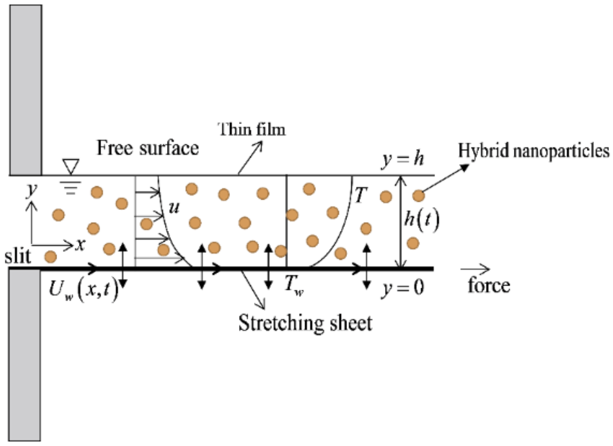

Fig. 1. Physical schematic [6].

$$u_x + v_y = 0 \tag{1}$$

$$\rho_{hnf}\left[u_t + uu_x + vu_y\right] = \mu_{hnf}u_{yy} \tag{2}$$

$$\left(\rho c_p\right)_{hnf}\left(T_t + uT_x + vT_y\right) = k_{hnf}T_{yy} \tag{3}$$

where u and v are velocity in x and y directions, respectively. ρ_{hnf} is the density of the hybrid nanofluids, the effective dynamic viscosity μ_{hnf} , k_{hnf} manifests the conduction due to the heat of nanodispersion and $\left(c_p\right)_{hnf}$ manifests the energy capacity of the nanodispersion. The problem is subjected to

$$\begin{aligned} &y = 0: \; u = U_w,\; v = V_w,\; T = T_w,\; y = h(t): \\ &u_y = T_y = 0,\; v = h'(t) \end{aligned} \tag{4}$$

where U_w and T_w are the surface velocity and the temperature of the stretching sheet respectively. The following transformations for nondimensional are introduced [6]:

$$\psi = \left[vb(1-\alpha t)^{-1}\right]^{\frac{1}{2}} x\beta f(\eta),$$
$$T = T_0 - T_{ref}\left(\frac{bx^2}{2v}\right)(1-\alpha t)^{-\frac{3}{2}}\theta(\eta) \tag{5}$$
$$\eta = \left(\frac{b}{v}\right)^{\frac{1}{2}}(1-\alpha t)^{-\frac{1}{2}}\beta^{-1}y$$

Here, $\psi(x,y,t)$ is the stream function and identically satisfies the continuity equation (1). Thin-film thickness is represented by β, where $\beta = b[\nu(1-\alpha t)]^{-\frac{1}{2}}h(t)$ and the changing of the thin-film thickness can be written as $h'(t) = -\frac{1}{2}\alpha\beta(\nu b^{-1})(1-\alpha t)^{-\frac{1}{2}}$. By imposing the equation (5) into the governing equations (1)-(3) along with the boundary conditions (4), we have,

$$\left(\frac{A_1}{A_2}\right)(f'''(\eta)) + \gamma\left[(f(\eta)f''(\eta)) - (f'(\eta))^2 - S\left(f'(\eta) + \frac{1}{2}\eta f''(\eta)\right)\right] = 0 \tag{6}$$

$$\left(\frac{A_3}{A_4}\right)\theta''(\eta) + \Pr\gamma\left[-S\left(\frac{3}{2}\theta(\eta) + \frac{1}{2}\eta\theta'(\eta)\right) - 2\left(f'(\eta)\theta(\eta)\right) + \left(f(\eta)\theta'(\eta)\right)\right] = 0 \tag{7}$$

$$f'(0) = 1,\ f(0) = w,\ f(1) = 0.5S,\ f''(1) = 0 \tag{8}$$

$$\theta(1) = 1,\ \theta'(1) = 0 \tag{9}$$

A_i $(i = 1,\ 2,\ 3,\ 4)$ is the thermophysical properties for the hybrid nanofluid. $S = \alpha b^{-1}$ measures the unsteadiness of the dimensionless and $\Pr = (\mu c_p)_{bf}\left(k_{bf}\right)^{-1}$ denotes the Prandtl number. The thermophysical characteristics of the hybrid nanofluid are demonstrated in [17] as follows.

$$A_1 : \rho_{hbf} = \left[\phi_1\rho_{s1} + \phi_2\rho_{s2} + (1-\phi_1)(1-\phi_2)\rho_{bf}\right]$$
$$A_2 : (\rho C_p)_{hrf} = \left[\phi_1(\rho C_p)_{s1} + \phi_2(\rho C_p)_{s2} + (1-\phi_1)(1-\phi_2)(\rho C_p)_{bf}\right]$$
$$A_3 : \mu_{hnf} = \frac{\mu_{bf}}{[1-(\phi_1+\phi_2)]^{2.5}}$$
$$A_4 : \frac{K_{hnf}}{K_{nf}} = \frac{K_{s2} + 2K_{nf} - 2\phi_2\left(K_{nf} - K_{s2}\right)}{K_{s2} + 2K_{nf} + \phi_2\left(K_{nf} - K_{s2}\right)} \text{ where } \frac{K_{nf}}{K_{bf}} = \frac{K_{s1} + 2K_{bf} - 2\phi_1\left(K_{bf} - K_{s1}\right)}{K_{s1} + 2K_{bf} + \phi_1\left(K_{bf} - K_{s1}\right)}$$

where ρ, ρC_p, μ and k and are density, heat capacity, dynamic viscosity, and thermal conductivity, respectively. The subscripts hnf, bf, s_1 and s_2 refer to the hybrid nanofluid, base fluid, the solid component for alumina and copper, accordingly. Also, ϕ_1 and ϕ_2 are the volume fraction of the nanoparticle alumina and copper. The characteristics of the hybrid nanofluids, copper and alumina as well as blood as base fluids are depicted in Table 1 [17, 18].

Fig. 1 shows an unsteady incompressible Newtonian fluid flows through the stretching sheet with wall transpiration at the boundary layer flow. It is important to derivate the physical quantities of the fluid flow behavior that can be a good reference to researchers or engineers in practical applications. In this research, the physical quantities are the local skin fraction, C_f which depicts the wall shear stress, $\tau_w(x)$ and the heat transfer rate $q_w(x)$ that is shown through the Nusselt number, Nu_x. The physical quantities are defined as

$$C_f = \frac{\tau_w(x)}{\rho_f u_w^2} \text{ and } Nu_x = \frac{xq_w(x)}{k_f(T_w - T_\infty)} \tag{10}$$

$\tau_w(x)$ and $q_w(x)$ in term of fluid is defined by Rehman et al. [19] as

$$\tau_w(x) = -\mu_{hnf}\left(1 + \frac{1}{\beta}\right)\left(\frac{\partial u}{\partial y}\right)_{y=0} \text{ and}$$
$$q_w(x) = -k_w\left(\frac{\partial T}{\partial y}\right)_{y=0} \tag{11}$$

Using similarity equation (6), the dimensionless local skin friction and heat transfer coefficient can be rewritten as

$$C_f \,\mathrm{Re}^{\frac{1}{2}} = \frac{1}{\delta}\left[\frac{1}{(1-\phi_1)^{2.5}+(1-\phi_2)^{2.5}}\right]\left(1+\frac{1}{\beta}\right) f''(0),$$
$$Nu_x \,\mathrm{Re}^{-\frac{1}{2}} = \frac{1}{\delta}\left(\frac{k_{hnf}}{k_f}\right)\theta'(0) \tag{12}$$

where Reynold number, $Re = \frac{xu_w}{V_f}$.

3. Results and discussion

By setting the Prandtl number, Pr=2.0363 [16] the solution of (6) and (7) associated with boundary conditions (8) and (9) can be obtained by using the bvp4c MATLAB solver. The relative tolerance has been fixed to 1×10^{-10} throughout the computational process. The effect of the unsteadiness parameter S and intensity of the constants mass transfer parameter w on the velocity and temperature profiles are graphically demonstrated and discussed. The values of the nanoparticles volume fraction have been fixed initially at $\phi_1 = 0.05$ for alumina and $\phi_2 = 0.04$ for copper concentrations. The legitimacy of the method is obtained by contrasting the current outcome and the past outcome. It can be seen in Table 2 that the numerical values are in good agreement with the results by Wang [6].

A non-uniqueness solution namely the first and second solutions have been identified when S and w varies. The first solution is the solution that converges asymptotically with a thin boundary layer while the second solution converges asymptotically with a thicker boundary layer. The positive value of the parameter S points out the accelerating fluid flow in a thin film. The effect of S and w on $C_f Re^{\frac{1}{2}}$ and $Nu_x Re^{-\frac{1}{2}}$ are depicted in Table 3. It is found that the growth of S escalates $C_f Re^{\frac{1}{2}}$ for both solutions. The increases of S tends to reduce the $Nu_x Re^{-\frac{1}{2}}$ in injection and first solution for the suction case. However, an opposite manner is observed for the first solution in the suction case.

Fig. 2a and 2b show the effect of S on the velocity distribution for the suction case, $w > 0$ and injection case, $w < 0$, respectively. There exist dual solutions for the accelerating fluid flow either in the suction case or injection case. The first solution reveals enhancement in velocity profile as S increases from 2.1 to 2.4 for the suction case. It remains the same pattern for the injection case. Meanwhile, the second solution is only obtained when $S = 2.3$ and $S = 2.4$ for the suction case and $S = 0.9$ to $S = 1.8$ for the injection case. The second solutions remain the same trend as the first solution for both cases. This phenomenon increases the wall shear stress and leads to a boosted-up momentum boundary layer in the fluid.

The effect of w on the velocity profile for the suction case is presented in Fig. 3a. The intensity of the suction escalates as w increases from 0.2 to 1.1. The enhancement of the parameter w illustrates the dominance of suction at the surface permeable stretching sheet. The presence of suction traps the hindering particles in the liquid system and slow-down the fluid flow over the stretching sheet. The increasing of w has reduced the local wall shear stress. The momentum boundary layer thickness becomes thinner as the suction effect is intensified. There is an enhancement in the velocity distribution for the injection case as shown in Fig. 3b. The intensity of the injection rises when the value of w decreases from -0.8 to -1.0. The velocity distribution is enlarged as w is increased. Besides, the thickness of the momentum boundary layer is slightly increased. The second solutions exist when $w = 0.2$, $w = -0.9$ and $w = -1.0$. The particles in the fluid moved faster with a larger injection effect.

Fig. 4a and 4b depict the trend of temperature distributions for the suction case and injection case respectively. The thickness of the thermal boundary layer becomes thicker since the temperature of the fluid increases as S improves from 2.1 to 2.4 in the first solution. This indicates that there is more heat transfer from the outside of the thin film to the hybrid nanofluid flow. The existence of the second solution on the temperature distribution for $S = 2.3$ and $S = 2.4$. A smaller thermal boundary layer thickness is noticed for $S = 2.4$. This opposite trend of the variations of the $S = 2.4$ on $\theta(0)$ for injection case is illustrated in Fig. 4b for both solutions.

Fig. 5a illustrates the temperature distribution decreases as the suction parameter increases from 0.2 to 1.1. However, there is an increment on $\theta(0)$ as w decreases from -0.8 to -1.0 for the injection case (see Fig. 5b). The given temperature profiles in Fig. 5a and 5b evident that the thermal boundary layer turns out to be thinner when the boundary of the thin film is sucked in compared to the injected one. The thermal gradient in the suction case is higher than in the injection case. Fig. 5 also depicts the second solution for both cases. It shows an opposite pattern for the second temperature solution in the injection case when compared with the first solution. The second solution in the suction case only exists at $w = 0.2$.

4. Conclusions

This research paper has investigated the issue of boundary layer flow and heat transfer in a thin film with an accelerating hybrid nanofluid flow over a porous stretching sheet. The behavior of the fluid is addressed and discussed graphically. There occur dual solutions for the velocity and

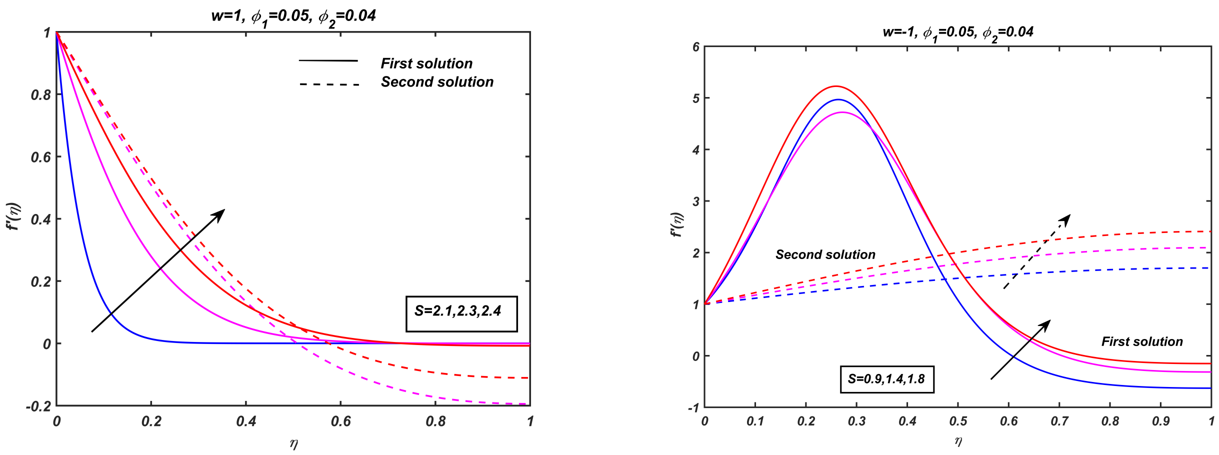

(a) (b)

Fig. 2. Effect of S on velocity for suction case (a) and injection case (b)

Table 2. Comparison of numerical results and analytical results for some values of S

S	Wang [6]			Present study		
	β	$f''(0)$	$\theta'(0)$	β	$f''(0)$	$\theta'(0)$
0.6	3.13125	-3.74233	-	3.13171	-3.74279	-0.14232
0.7	2.57701	-3.14965	-	2.57600	-3.14961	-0.11301
0.8	2.15199	-2.68094	0.09047	2.15199	-2.68097	-0.09047
1.0	1.54362	-1.97238	-	1.54342	-1.97239	-0.05860

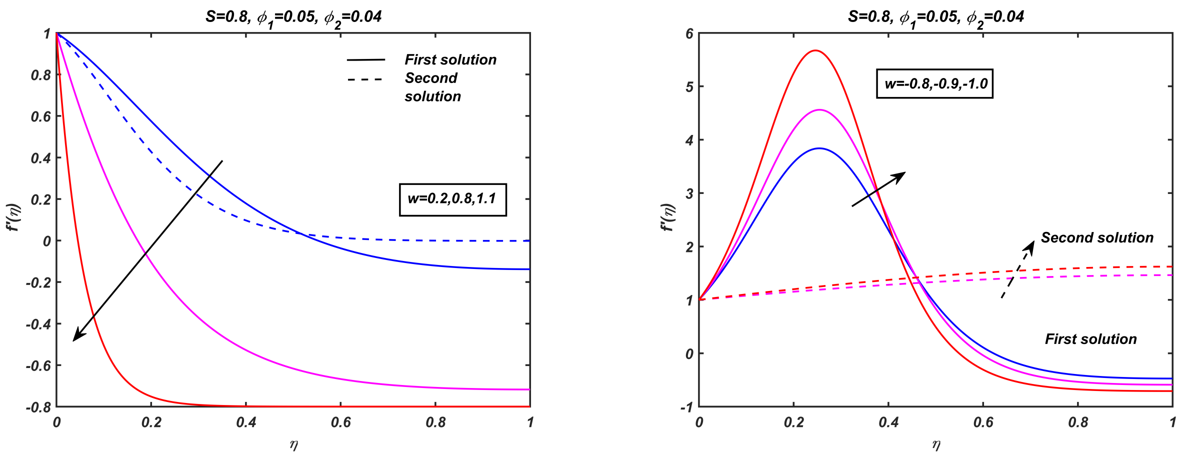

(a) (b)

Fig. 3. Effect of w on velocity for suction case (a) and injection case (b)

temperature profiles in either suction or injection situations. The velocity profiles are enhanced in both solutions as S increases for both suction and injection cases. There is a reduction in the velocity field in the suction case but an opposite manner is noticed for the injection case when the constants mass transfer parameter w is enlarged. S has increased the temperature distribution in the first solution for the suction case but the profiles are diminished in the second solution for the injection case. The increment of mass transfer parameter w has declined the temperature profile in the first solution (suction case) and the second solution (injection case). However, a different trend is observed for the first temperature solution in the injection case.

Table 3. Values for local skin friction, $C_f Re^{\frac{1}{2}}$ and Nusselt number $Nu_x Re^{-\frac{1}{2}}$ for various number of S and w

Parameters	Cases		$C_f Re^{\frac{1}{2}}$		$Nu_x Re^{-\frac{1}{2}}$	
	Suction	Injection	First solution	Second solution	First solution	Second solution
S	2.1	-	-18.4878	-	-31.5109	-
	2.3	-	-5.0994	-2.5020	-12.1070	-5.2030
	2.4	-	-3.2838	-2.3445	-9.1614	-5.8770
	-	0.9	10.5245	1.1551	-3.7924	-1.1324
	-	1.4	12.2527	1.7577	-4.1574	-1.2810
	-	1.8	15.6161	2.2394	-4.5661	-1.3553
w	0.2	-	-1.5385	-6.4191	-1.9795	-11.242
	0.8	-	-7.8867	-9.1644	-	-
	1.1	-	-31.6180	-25.9819	-	-
	-	-0.8	9.5175	-	-4.2214	-
	-	-0.9	10.2486	0.8010	-3.9863	-1.0894
	-	-1.1	11.5126	1.0339	-3.8162	-0.9822

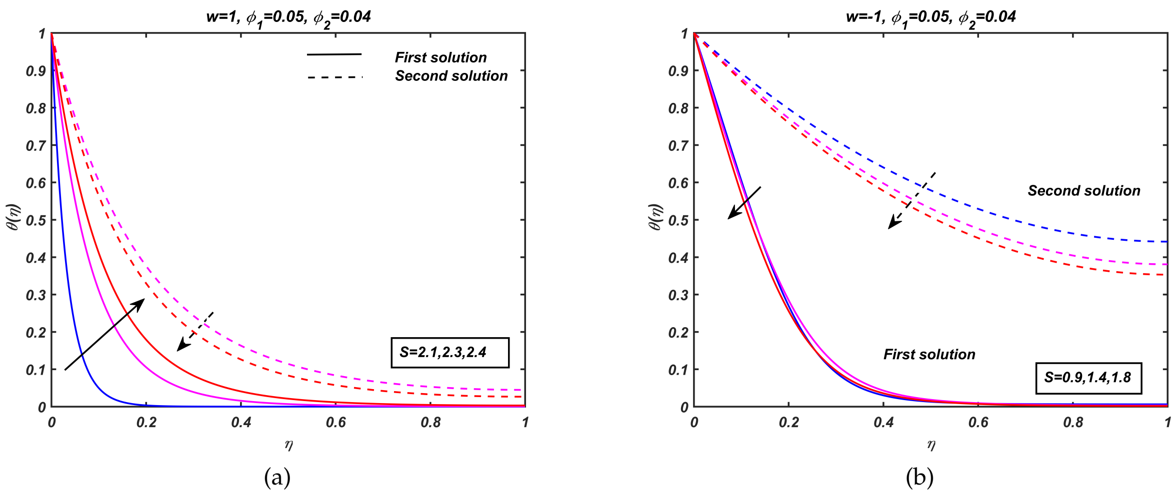

Fig. 4. Effect of S on temperature for suction case (a) and injection case (b)

Acknowledgments

The authors would like to acknowledge the Ministry of Higher Education Malaysia for financial support through vote numbers FRGS/1/2019/STG06/UTM/02/4.

References

[1] L. J. Crane, (1970) *"Flow past a stretching plate"* **Zeitschrift für angewandte Mathematik und Physik ZAMP** *21*(4): 645–647.

[2] P. Carragher, C. LJ, et al., (1982) *"Heat transfer on a continuous stretching sheet"*:

[3] B. Sakiadis, (1961) *"Boundary-layer behavior on continuous solid surfaces: II. The boundary layer on a continuous flat surface"* **AiChE journal** *7*(2): 221–225.

[4] C. Wang, (1990) *"Liquid film on an unsteady stretching surface"* **Quarterly of applied Mathematics** *48*(4): 601–610.

[5] H. I. Andersson, J. B. Aarseth, and B. S. Dandapat, (2000) *"Heat transfer in a liquid film on an unsteady stretching surface"* **International Journal of Heat and Mass Transfer** *43*(1): 69–74.

[6] C. Wang, (2006) *"Analytic solutions for a liquid film on an unsteady stretching surface"* **Heat and Mass Transfer** *42*(8): 759–766.

[7] I.-C. Liu and H. I. Andersson, (2008) *"Heat transfer in a liquid film on an unsteady stretching sheet"* **International Journal of Thermal Sciences** *47*(6): 766–772.

[8] P. G. Metri, J. Tawade, and M. S. Abel, (2016) *"Thin film flow and heat transfer over an unsteady stretching sheet with thermal radiation, internal heating in presence of external magnetic field"* **arXiv preprint arXiv:1603.03664**:

[9] R. Usha and R. Sridharan, (1993) *"On the motion of a liquid film on an unsteady stretching surface"* **ASME-PUBLICATIONS-FED** *150*: 43–43.

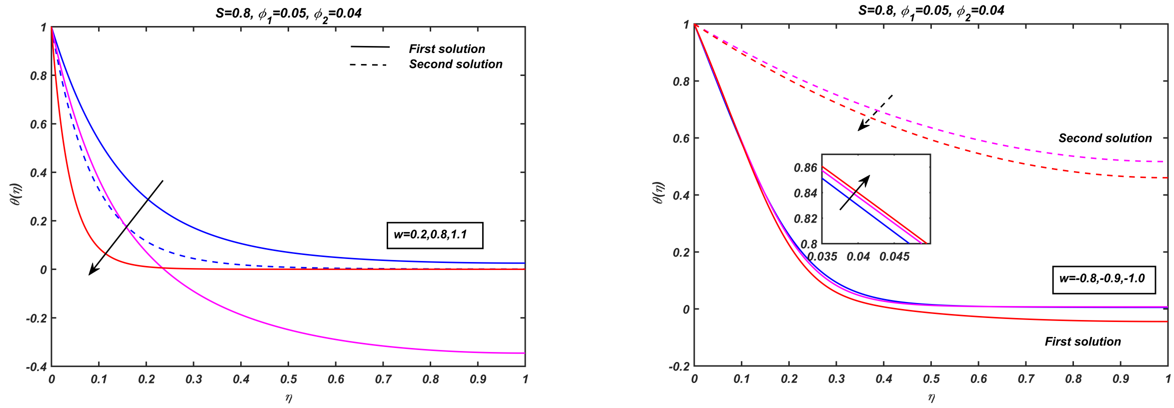

(a) (b)

Fig. 5. Effect of w on temperature for suction case (a) and injection case (b)

[10] R. C. Aziz, I. Hashim, and A. Alomari, (2011) *"Thin film flow and heat transfer on an unsteady stretching sheet with internal heating"* **Meccanica *46***(2): 349–357.

[11] B. Santra and B. S. Dandapat, (2009) *"Unsteady thin-film flow over a heated stretching sheet"* **International Journal of Heat and Mass Transfer *52***(7-8): 1965–1970.

[12] M. Qasim, Z. Khan, R. Lopez, and W. Khan, (2016) *"Heat and mass transfer in nanofluid thin film over an unsteady stretching sheet using Buongiorno's model"* **The European Physical Journal Plus *131***(1): 1–11.

[13] N. A. C. Sidik, I. M. Adamu, M. M. Jamil, G. Kefayati, R. Mamat, and G. Najafi, (2016) *"Recent progress on hybrid nanofluids in heat transfer applications: a comprehensive review"* **International Communications in Heat and Mass Transfer *78***: 68–79.

[14] O. Afonso and P. B. Vasconcelos. *Computational economics: A concise introduction*. Routledge, 2015.

[15] C. Sulochana and N. Sandeep, (2016) *"Stagnation point flow and heat transfer behavior of Cu–water nanofluid towards horizontal and exponentially stretching/shrinking cylinders"* **Applied Nanoscience *6***(3): 451–459.

[16] N. S. Akbar, D. Tripathi, and Z. H. Khan, (2018) *"Numerical simulation of nanoparticles with variable viscosity over a stretching sheet"* **Numerical Simulations in Engineering and Science**:

[17] I. Waini, A. Ishak, and I. Pop, (2020) *"MHD flow and heat transfer of a hybrid nanofluid past a permeable stretching/shrinking wedge"* **Applied Mathematics and Mechanics *41***(3): 507–520.

[18] A. Kamyar, R. Saidur, and M. Hasanuzzaman, (2012) *"Application of computational fluid dynamics (CFD) for nanofluids"* **International Journal of Heat and Mass Transfer *55***(15-16): 4104–4115.

[19] S. Rehman, M. Idrees, R. A. Shah, and Z. Khan, (2019) *"Suction/injection effects on an unsteady MHD Casson thin film flow with slip and uniform thickness over a stretching sheet along variable flow properties"* **Boundary Value Problems *2019***(1): 1–24.